pp 169-224, Academic Press, New York.
Goyne, T. E., & Sigman, D. S. (1987) *J. Am. Chem. Soc. 109*, 2846-2848.
Kappen, L. S., & Goldberg, I. H. (1989) *Biochemistry 28*, 1027-1032.
LeClerc, J. E., Istock, N. L., Saran, B. R., & Allen, R., Jr. (1984) *J. Mol. Biol. 180*, 217-237.
Miller, J. H. (1985) *J. Mol. Biol. 182*, 45-68.
Montenary-Garestier, T., Charlier, M., & Hélène, C. (1976) in *Photochemistry and Photobiology of Nucleic Acids* (Wang, S. Y., Ed.) Vol. I, pp 381-417, Academic Press, New York.
Povirk, L. F., & Goldberg, I. H. (1985) *Proc. Natl. Acad. Sci. U.S.A. 82*, 3182-3186.
Povirk, L. F., & Goldberg, I. H. (1986) *Nucleic Acids Res. 14*, 1417-1426.
Povirk, L. F., Houlgrave, C. W., & Han, Y.-H. (1988) *J. Biol. Chem. 263*, 19263-19266.
Rahn, R. O., & Patrick, M. H. (1976) in *Photochemistry and Photobiology of Nucleic Acids* (Wang, S. Y., Ed.) Vol. II, pp 97-145, Academic Press, New York.
Rhaese, H.-J., & Freese, E. (1968) *Biochim. Biophys. Acta 155*, 476-490.
Schulte-Frohlinde, D., Opitz, J., Görner, H., & Bothe, E. (1985) *Int. J. Radiat. Biol. 48*, 397-408.
Uesugi, S., Shida, T., & Ikehara, M. (1981) *Chem. Pharm. Bull. 29*, 3573-3585.
Vodička, P., & Hemminki, K. (1988) *Chem.-Biol. Interact. 68*, 153-164.
Wang, S. Y. (1976) in *Photochemistry and Photobiology of Nucleic Acids* (Wang, S. Y., Ed.) Vol. I, pp 295-356, Academic Press, New York.

Anisotropic ^2H NMR Spin-Lattice Relaxation in L_α-Phase Cerebroside Bilayers†

Julia B. Speyer, Ralph T. Weber, Sunil K. Das Gupta, and Robert G. Griffin*

Francis Bitter National Magnet Laboratory and Department of Chemistry, Massachusetts Institute of Technology, Cambridge, Massachusetts 02139

Received August 21, 1989; Revised Manuscript Received October 5, 1989

ABSTRACT: A series of ^2H NMR inversion recovery experiments in the L_α phase of the cerebroside *N*-palmitoylgalactosylsphingosine (NPGS) have been performed. In these liquid crystalline lipid bilayers we have observed substantial anisotropy in the spin-lattice relaxation of the CD_2 groups in the acyl chains. The form and magnitude of the anisotropy varies with position in the chain, being positive in the upper region, decreasing to zero at the 4-position, and reversing sign at the lower chain positions. It is also shown that addition of cholesterol to the bilayer results in profound changes in the anisotropy. These observations are accounted for by a simple motional model of discrete hops among nine sites, which result from the coupling of two modes of motion—long-axis rotational diffusion and gauche-trans isomerization. This model is employed in quantitative simulations of the spectral line shapes and permits determination of site populations and motional rates. These results, plus preliminary results in sphingomyelin and lecithin bilayers, illustrate the utility of T_1 anisotropy measurements as a probe of dynamics in L_α-phase bilayers.

Solid-state ^2H NMR[1] has contributed substantially toward understanding the phase behavior and dynamic structure of lipid bilayers, the fundamental structural unit of membranes. To date, the most complete descriptions of lipid dynamics have been of the gel phase, because in this phase lipid molecules execute motions that are within the range of intermediate exchange rates for ^2H NMR ($10^{-7} < \tau_c < 10^{-3}$ s). The spectra are therefore sensitive to changes in the motional rates and mechanisms, and a detailed description of the dynamic processes can be extracted from simulations of the quadrupole echo line shapes and their dependence on temperature and pulse separation (Wittebort et al., 1987; Blume et al., 1982; Huang et al., 1980; Meier et al., 1983, 1986).

Although the L_α or liquid crystalline phase of lipid bilayers is an excellent model for many biological membranes, it has been less well characterized because the motions in this phase occur at rates which fall into the fast-limit regime ($\tau_c < 10^{-7}$ s), where the ^2H line shapes are insensitive to variations in the rate (Spiess & Sillescu, 1981; Wittebort et al., 1987). Thus, quadrupole echo spectra of liquid crystalline bilayers are motionally narrowed, axially symmetric Pake patterns with the splittings between the perpendicular edges of the powder patterns, $\Delta\nu_{Q\perp}$, dependent not on the rate of motion but rather on the averaged orientation of the C-D bond with respect to the axis of motion (Charvolin et al., 1973; Seelig & Seelig, 1974). As the splitting is essentially the only variable feature in these line shapes, they are generally interpreted in terms of order parameters, S_{CD}, which indicate the average orientation of the C-D segments with respect to the bilayer normal through the relation (Seelig & Seelig, 1974; Seelig, 1977)

$$\Delta\nu_{Q\perp} = \frac{3}{4}\frac{e^2qQ}{h}S_{CD} \quad (1a)$$

$$S_{CD} = (1/2)(3\overline{\cos^2\theta} - 1) \quad (1b)$$

† This research was supported by the National Institutes of Health (GM-25505 and RR-00995).

[1] Abbreviations: CHOL, cholesterol; DMPC, 1,2-dimyristoyl-*sn*-phosphatidylcholine; DPPC, 1,2-dipalmitoyl-*sn*-phosphatidylcholine; DPPE, 1,2-dipalmitoyl-*sn*-phosphatidylethanolamine; efg, electric field gradient; NMR, nuclear magnetic resonance; NPGS, *N*-palmitoylgalactosylsphingosine; NPSM, *N*-palmitoylsphingomyelin; PC, phosphatidylcholine; SUV, small unilamellar vesicles.

0006-2960/89/0428-9569$01.50/0

where $e^2qQ/h \sim 167$ kHz, the rigid lattice quadrupole coupling for a C–D bond, and the bar denotes the equilibrium spatial average of θ, the angle between the C–D bond vector and the bilayer normal. Although measurement of order parameters and order profiles has provided meaningful insights into the dynamic structure of the L_α phase (Seelig & Seelig, 1974; Davis, 1983), it has not been possible to obtain information on the mechanism or the rates of motion which lead to the narrowing. Thus, many aspects of the dynamic properties of bilayer membranes have remained uncharacterized.

The spin–lattice relaxation time, T_1, is sensitive to motions with rates near the Larmor frequency, and as a consequence can provide information on faster motions which are inaccessible through quadrupole echo line shapes. Furthermore, T_1 is dependent on the molecular orientation with respect to the magnetic field, and this dependence is sensitive to motional mechanisms as well as to motional rates (Doane et al., 1974; Torchia & Szabo, 1982; Siminovitch et al., 1985, 1988). It should be possible, therefore, to employ models of fast motion suitable for simulating spin–lattice relaxation behavior in a spirit similar to the intermediate time scale motional models used in simulating quadrupole echo line shapes. This approach was effectively applied in analyzing the two-site motion of water molecules in barium chlorate monohydrate (Griffin et al., 1988) and of aromatic rings (Hiyama et al., 1986; Rice et al., 1987) and the three-site hopping motion of methyl groups (Batchelder et al., 1983; Beshah et al., 1987; Beshah & Griffin, 1989). In the gel phase, T_1 anisotropy in oriented samples was used to determine motions of the lipid backbone in a glycerol-based glycolipid (Auger et al., 1989). However, most ^2H relaxation studies of L_α-phase lipid bilayers have been confined to analysis of the dependence of T_1 on temperature (Meier et al., 1986; Mayer et al., 1988), chain position (Brown et al., 1983; Williams et al., 1985), or magnetic field strength (Brown et al., 1983).

The potential application of orientation-dependent T_1's as a probe of L_α-phase lipid dynamics has yet to be realized, since it has been thought that the T_1 anisotropy of L_α-phase liposomes is masked by the orientational averaging effects of rapid lateral diffusion. Specifically, it has been suggested that the lateral diffusion in L_α-phase PC bilayers is sufficiently rapid, and that the liposome curvature is sufficiently small, to enable the lipid molecule to experience a large range of orientations with respect to the magnetic field within the relaxation time, T_1 (Brown & Davis, 1981). In such a case, inversion recovery experiments using randomly oriented samples would not exhibit a T_1 anisotropy. More recently, Jarrell et al. (1988) have demonstrated that even with oriented PC bilayers the fatty acyl chains still exhibit negligible T_1 anisotropy in the L_α phase. Because of the negative results of these two experiments, there has been little active searching for anisotropic T_1's in any L_α-phase lipid other than lecithin. Nevertheless, Siminovitch et al. (1985, 1988) reported that liquid-gelatin (Blume & Griffin, 1982) liposomes containing CHOL exhibit a clear T_1 anisotropy, both in the hydrocarbon chains and in the sterol. Orientational averaging from rapid lateral diffusion presumably is not effective in suppressing T_1 anisotropies because CHOL decreases the lateral diffusion rates and/or increases the liposome size.

We report here our studies of the cerebroside NPGS in the L_α phase. We have observed anisotropic spin–lattice relaxation in L_α-phase liposomes of selectively deuterated NPGS at the 3-, 4-, 5-, 7-, and 12-positions of the palmitoyl chain.[2] The

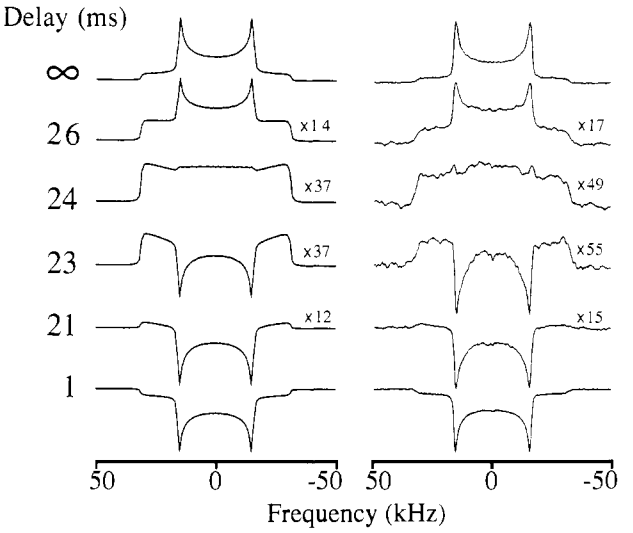

FIGURE 1: (Right) ^2H NMR inversion recovery spectra of 3,3-d_2-NPGS bilayers at 87 °C displayed as a function of the relaxation delay t, between a 180° inverting pulse and acquisition with a quadrupolar echo. Spectra near the zero crossing are expanded vertically as indicated. The partially recovered line shapes exhibit T_1 anisotropy across the powder pattern which can be simulated (left) with a nine-site hopping model of long-axis rotational diffusion coupled with gauche–trans isomerization as described in the text. The axial diffusion is accomplished by three 120° hops about the long axis with a jump rate, k_{ax}, of 2×10^9 s^{-1}, corresponding to a rotational diffusion rate, D, of 8.8×10^9 s^{-1} from $D = (4\pi^2/N^2)k$, where N is the number of sites (Torchia & Szabo, 1982). The two gauche sites are equally populated, and the population of the trans site ($P_t = 0.5$) is chosen so that the simulations reproduce the observed quadrupolar splitting, $\Delta\nu_{Q\perp}$, of 31.5 kHz. The gauche–trans isomerization rate, k_{gt}, is 3.74×10^9 s^{-1}. The T_1 values at various orientations are obtained from the simulations. Specifically, $T_1(90°) = 35.1$ ms, $T_1(54.7°) = 32.7$ ms, and $T_1(0°) = 28.7$ ms to yield $\Delta T_1 = 0.41$.

form and extent of the T_1 anisotropies are dependent on chain position and on the presence or absence of CHOL. We have found that the spectra can be consistently simulated with a discrete hopping model of gauche–trans isomerization, combined with three-site axial diffusion. As will be seen below, the detailed success of this nine-site model is quite striking.

Results

To examine T_1 anisotropies in cerebrosides, we have performed inversion recovery experiments[3] on NPGS samples labeled at the 3-, 4-, 5-, 7-, and 12-positions. The T_1 anisotropy is most apparent near the zero crossing [$t = T_1(\ln 2)$] where

[2] Sample Preparation: NPGS was synthesized according to the method of Radin (1972) using palmitic acids selectively deuterated at the 3-, 4-, 5-, 7-, or 12-position (Das Gupta et al., 1982). The 12,12-d_2-NPGS/CHOL sample was prepared as described previously (Siminovitch et al., 1988). All samples consisted of approximately 70 mg of labeled lipid dispersed in deuterium-depleted water (~70 wt % H_2O) sealed in 7-mm glass tubes under vacuum. Dispersion was completed by heating the samples above the gel to liquid crystalline phase transition [$T_c = 82$ °C for pure NPGS or $T_c = 70$ °C for 45 mol % CHOL (Ruocco & Shipley, 1984)] for about 2 h.

[3] ^2H NMR Spectroscopy: Spectra were obtained at 61.0 MHz with an inversion recovery sequence (180_x–t–90_x–τ–90_y–τ–ACQ) described previously (Siminovitch et al., 1985, 1988). The pulse spacing τ was 30 μs, and the $\pi/2$ pulse length was ≤2.1 μs. The recycle delay was at least 5 times the T_1 of the slowest recovering orientation. The number of acquisitions for each spectrum varied from 2000 to 64 000 depending on the proximity to the zero crossing [when the relaxation interval $t \sim T_1(\ln 2)$] where the spectral intensity is exceedingly low. Finite pulse effects (Bloom et al., 1980) on the line shapes were minimal since pulse lengths were short but were nevertheless accounted for in the simulations. The temperature was kept constant to within 0.5 °C during the experiments by blowing heated air into an insulated chamber housing the rf sample coil.

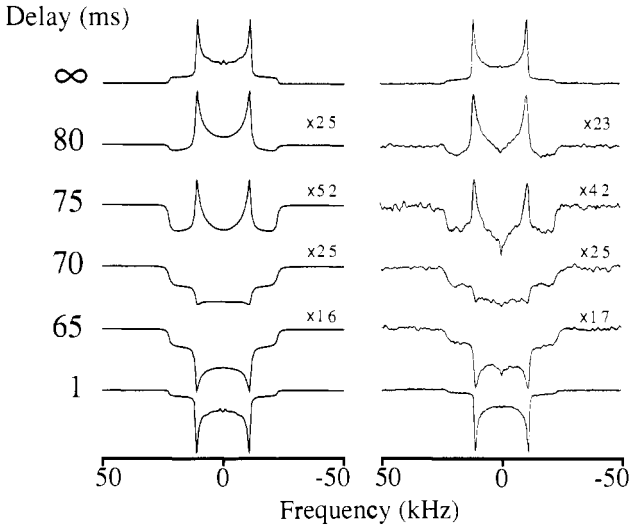

FIGURE 2: (Right) ^{2}H NMR inversion recovery spectra of 12,12-d_2-NPGS bilayers at 87 °C displayed as a function of the relaxation delay time, t, and compared with spectral simulations (left). The quadrupole splitting is $\Delta\nu_{Q\perp}$ = 22.5 kHz. By use of the nine-site model described in the text and in the caption to Figure 1, the simulations were executed with the following parameters: $P_t = 0.36$; $P_{g^+} = P_{g^-} = 0.32$; $k_{gt} = 6 \times 10^{10}$ s^{-1}; $k_{ax} = 2 \times 10^9$ s^{-1} ($D = 8.8 \times 10^9$ s^{-1}). T_1 values obtained from the simulations: $T_1(90°) = 105$ ms, $T_1(54.7°) = 112$ ms, $T_1(0°) = 131$ ms, and $\Delta T_1 = -0.45$.

some parts of the powder pattern are positive in intensity, while other parts are still negative, as is illustrated in Figures 1–3. As a measure of the T_1 anisotropy, we define ΔT_1 (for an $\eta = 0$ line shape) as

$$\Delta T_1 = T_1(90°)/T_1(0°) - T_1(0°)/T_1(90°) \qquad (2)$$

where 0° and 90° correspond to the parallel and perpendicular edges of the spectrum. Thus, if the spin–lattice relaxation is uniform across the powder pattern, then $\Delta T_1 = 0$, whereas if the parallel or perpendicular edges relax more rapidly then $\Delta T_1 > 0$ or $\Delta T_1 < 0$, respectively.

Figures 1 and 2 show spectra of pure 3,3-d_2-NPGS and 12,12-d_2-NPGS bilayers at 87 °C, and Figure 3 shows spectra of 12,12-d_2-NPGS + 40 mol % CHOL at 75 °C. At the top of each figure is a fully relaxed quadrupole echo spectrum in the form of an axially symmetric Pake pattern. The difference among the three lies in the breadth of the Pake patterns, as indicated by the quadrupole splittings given in the figure captions. Although the fully relaxed quadrupole echo spectra all have identical line shapes, a glance at the partially recovered spectra immediately shows distinctions among the three in relaxation behavior.

All three samples show an obvious T_1 anisotropy, but the form of the anisotropy differs among the samples. For deuterons at the 3-position near the top of the NPGS chain (Figure 1), the parallel edges recover faster ($\Delta T_1 > 0$), whereas at the 12-position (Figure 2) the T_1 anisotropy is reversed, so that the perpendicular edges of the powder pattern recover more rapidly ($\Delta T_1 < 0$). The chain positions intermediate between 3 and 12 also show anisotropic behavior which varies along the length of the chain. While at position 3 ΔT_1 is positive, at position 4 (not shown) $\Delta T_1 \simeq 0$ (the anisotropy vanishes), and at position 5 and beyond it reverses sign.

The addition of CHOL to the bilayer can significantly alter the form of the anisotropy at a particular position. This can be seen by comparing Figures 2 and 3, where the inversion recovery line shapes of 12,12-d_2-NPGS in the absence and presence of 40% CHOL are shown, respectively. In the presence of CHOL the anisotropy in the relaxation reverses

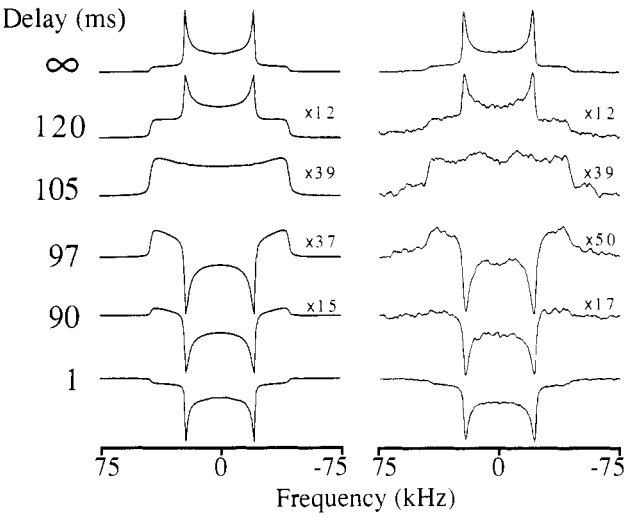

FIGURE 3: (Right) ^{2}H NMR inversion recovery spectra of 60% 12,12-d_2-NPGS/40% CHOL bilayers at 75 °C displayed as a function of the relaxation delay time, t, and compared with spectral simulations (left). The addition of cholesterol significantly increases the trans population as reflected by the increased quadrupole splitting of $\Delta\nu_{Q\perp}$ = 43.1 kHz. By use of the nine-site model described in the text and in the caption to Figure 1, the simulations were executed with the following parameters: $P_t = 0.688$; $P_{g^+} = P_{g^-} = 0.156$; $k_{gt} = 4.4 \times 10^9$ s^{-1}; $k_{ax} = 1.75 \times 10^{10}$ s^{-1} ($D = 7.7 \times 10^{10}$ s^{-1}). T_1 values obtained from the simulations: $T_1(90°) = 156$ ms, $T_1(54.7°) = 142$ ms, $T_1(0°) = 121$ ms, and $\Delta T_1 = 0.51$.

sign, and $\Delta T_1 > 0$, analogous to the case of 3,3-d_2-NPGS (Figure 1). A similar reversal has been recorded for 7,7-d_2-NPGS. As reported previously, L_α-phase NPGS bilayers containing CHOL exhibit $\Delta T_1 > 0$ at the 7-position (Siminovitch et al., 1988), and we have found $\Delta T_1 < 0$ at the 7-position in pure NPGS bilayers.

Discussion

Spectral Calculations. The time scale of the motions in the L_α phase ($\tau_c \ll \omega_Q^{-1}$) lends itself to use of the fast-limit approximation. In this case, calculation of the spectrum is simplified because the line shape depends solely on the equilibrium distribution of molecular orientations (Wittebort et al., 1987). The rapid diffusion about the lipid long axis leads to a motionally averaged efg tensor, $\bar{\mathbf{V}}$, with axial symmetry such that the powder line shape and the spin–lattice relaxation will exhibit a θ dependence, but not ϕ dependence (Torchia & Szabo, 1982), where θ and ϕ are the spherical polar angles that define the direction of the external magnetic field with respect to the principal axes of $\bar{\mathbf{V}}$. To simulate the inversion recovery experiments, the ^{2}H relaxation rate is calculated from

$$\frac{1}{T_1} = \frac{1}{3}\omega_Q^2[J_1(\omega_o) + 4J_2(2\omega_o)] \qquad (3)$$

where $\omega_Q = (3/4)e^2qQ/h$. The spectral density functions, J_1 and J_2, are obtained from Fourier analysis of the autocorrelation functions, $C_m(t)$, which are calculated according to the method of Torchia and Szabo (1982) and give rise to the orientation dependence of T_1. T_1 is calculated at each orientation of the external magnetic field, and the intensity is then weighted in proportion to $1 - 2e^{-t/T_1}$ in the powder pattern integration.

Significant gains in computational efficiency, compared to previous simulation programs in our laboratory (Wittebort et al., 1987), were achieved by recognizing that the part of the autocorrelation function which describes the motion of the quadrupole coupling symmetry axis is independent of the orientation of the external magnetic field (Torchia & Szabo,

1982). This function then needs to be calculated only once, making the time for computing T_1 at all orientations of the external magnetic field in the powder average essentially independent of the number of sites.

Dynamic Model. In simulating the partially recovered spectra we have used a simple discrete hopping model consisting of rotational diffusion via three 120° hops about the molecular long axis, coupled with gauche–trans tetrahedral hopping among three sites (t, g^+, and g^-), for a total of nine sites. All rates are in the fast limit on the ^2H NMR time scale ($\tau_c < 10^{-7}$ s), and therefore, the resulting line shape is an axially symmetric Pake pattern. The two gauche sites are equally populated in our model, and the population of the trans site is adjusted to match the splittings of the experimental spectra. As can be seen in Figures 1–3, the model accurately reproduces the anisotropy in the partially recovered line shapes at the different delays.

Despite its success, the model is a simplification of actual lipid dynamics. For instance, the polymethylene chains of a lipid molecule may assume a large number of configurations. The three possible CD_2 orientations of the model are therefore an approximation in which the rates reflect the sum of all possible paths from one site to another, rather than one distinct process. The motion is further simplified in that the long-axis diffusion is reasonably represented by jumps, rather than continuous diffusion. This is consistent with previous lineshape simulations of gel phase (Blume et al., 1982) and liquid gelatin phase lipid bilayers (Siminovitch et al., 1988). In addition, spin–lattice relaxation spectra of ^2H-labeled CHOL in PC bilayers have been simulated more accurately by 3-fold hops about the director rather than continuous diffusion (Bonmatin et al., 1988, 1989). Therefore, large-angle hopping appears to be a physically reasonable approximation for rotational diffusion about the director. Contrary to other motional models proposed for L_α-phase lipids (Meier et al., 1986; Mayer et al., 1988), we have not included in our calculation any wobble of the director with respect to the bilayer normal. The simulations indicate that this is not necessary, and evidence suggests that the amount of wobble is not significant in L_α-phase bilayers. In the case of NPGS bilayers, the breadth of the $^{13}C{=}O$ powder pattern of the carboxamide is essentially temperature independent from 70 to 90 °C (T. H. Huang, private communication), whereas fluctuations about the director would be expected to narrow the breadth of the powder pattern. Similarly, the quadrupole splitting of a glycerol backbone label in DPPC (R. Haberkorn, R. G. Griffin, and J. Seelig, unpublished results) and other glycerol phospholipids (Gally et al., 1981) shows only ~5% change over a 40 °C temperature range.

Once the geometry of our model is chosen, there are three variable parameters which must be specified: the trans population, the axial diffusion rate, and the gauche–trans isomerization rate. Also, there are three criteria to satisfy in fitting the experimental spectra—i.e., the simulation must reproduce the quadrupole splitting, the form of the T_1 anisotropy, and the relaxation times. The trans-site population determines the residual quadrupole splitting, and the two hopping rates are varied to reproduce the partially relaxed line shapes and the value of T_1. Of course, at any temperature all chain positions in the molecule must have the same axial diffusion rates, and this constrains the simulation parameters when spectra from multiple sites are analyzed simultaneously. In simulating the spectra from the 3- and 12-positions of NPGS, we have fulfilled this condition and maintained constant axial diffusion rates.

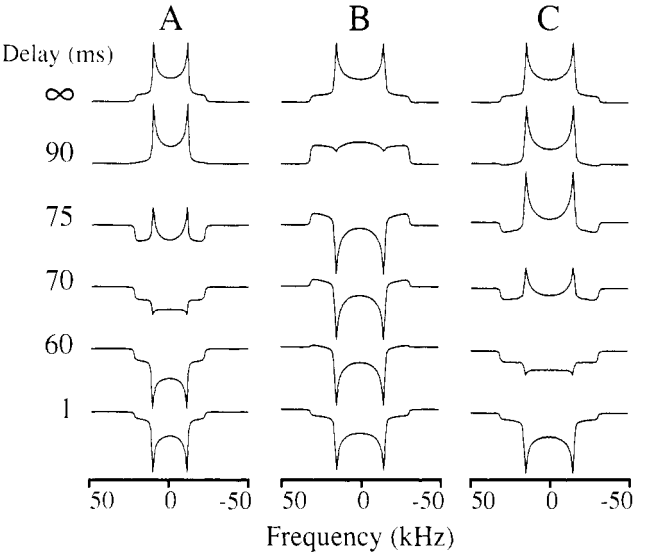

FIGURE 4: Three sets of inversion recovery simulations showing the effects of changing the trans population (A and B) or the relative rates of rotational diffusion and gauche–trans isomerization (B and C). The parameters for the three simulations are as follows: (A) P_t = 0.36, $P_{g^+} = P_{g^-}$ = 0.32, $\Delta\nu_{Q\perp}$ = 22.5 kHz, $k_{gt} = 6 \times 10^{10}$ s^{-1}, $k_{ax} = 2 \times 10^9$ s^{-1}, $T_1(0°)$ = 131 ms, $T_1(90°)$ = 105 ms, and ΔT_1 = −0.45; (B) P_t = 0.5, $P_{g^+} = P_{g^-}$ = 0.25, $\Delta\nu_{Q\perp}$ = 31.3 kHz, $k_{gt} = 6 \times 10^{10}$ s^{-1}, $k_{ax} = 2 \times 10^9$ s^{-1}, $T_1(0°)$ = 81.8 ms, $T_1(90°)$ = 134 ms, and ΔT_1 = 1.03; (C) P_t = 0.5, $P_{g^+} = P_{g^-}$ = 0.25, $\Delta\nu_{Q\perp}$ = 31.3 kHz, $k_{gt} = 6 \times 10^9$ s^{-1}, $k_{ax} = 2 \times 10^{10}$ s^{-1}, $T_1(0°)$ = 150 ms, $T_1(90°)$ = 92.6 ms, and ΔT_1 = −1.00. In (A) and (B) the rates are the same, but the trans population is increased in (B), causing a larger quadrupolar splitting in (B) and a positive ΔT_1. In (B) and (C) the populations are held the same, but the axial diffusion rate is slower than the gauche–trans isomerization rate in (B) and faster in (C). Increasing k_{ax} relative to k_{gt} causes the ΔT_1 to reverse sign and become negative.

Comparison of Results. The rates and populations drawn from simulations of the spectra are given in the figure captions. In pure NPGS bilayers the axial diffusion rate k_{ax} is 2×10^9 s^{-1}, corresponding to a correlation time τ_{ax} of $(3k_{ax})^{-1} = 0.2$ ns. The correlation times associated with gauche–trans isomerization are $\tau_{gt} = 9 \times 10^{-11}$ and 5×10^{-12} s at the 3- and 12-positions, respectively. Published correlation times of L_α-phase lipid are almost exclusively of DMPC or DPPC, and they span a large range of values reflecting the variety of techniques and models used in the several reports. Axial diffusion in DMPC has been examined with spin–lattice relaxation in ^{13}C NMR (Fuson & Prestegard, 1983) and ^1H NMR (Petersen & Chan, 1977) and found to occur with τ_{ax} = 20 ns, whereas EPR line shape (Lange et al., 1985) and ^2H (Mayer et al., 1988) and ^1H (Rommel et al., 1988) relaxation studies yield τ_{ax} = 1–7 ns. Similarly, Petersen and Chan (1977) have reported gauche–trans correlation times in DMPC of $\tau_{gt} \sim 10^{-9}$ to 2×10^{-10} s, but by ^2H T_1 relaxation, $\tau_{gt} = 5 \times 10^{-10}$ to 10^{-12} s in DMPC (Mayer et al., 1988) and τ_{gt} = 0.5 to 3×10^{-11} s in DPPC (Brown, 1982). Comparison of these results shows that, though the motions are generally faster in NPGS than in lecithins, our results are in closest agreement with the recent studies of Kothe and co-workers (Mayer et al., 1988; Rommel et al., 1988). Furthermore, in all cases internal motions such as gauche–trans isomerization are found to be about an order of magnitude faster than axial diffusion.

T_1 Anisotropy. The change in the sign of ΔT_1 may arise by at least two different mechanisms. First, if the two motional rates, k_{ax} and k_{gt}, are kept constant, but the trans population increases, the T_1 anisotropy becomes more positive. This scenario is illustrated in Figure 4A,B. The second mechanism involves varying the relative rates of axial diffusion and

gauche–trans isomerization, while holding the trans population constant, and is illustrated in Figure 4B,C. As the long-axis diffusion rate is increased relative to the gauche–trans rate, ΔT_1 becomes more negative.

The importance of both of these schemes can be appreciated by considering the sign reversal in ΔT_1 accompanying the addition of CHOL to [12,12-d_2]NPGS bilayers (Figures 2 and 3). The first mechanism seems to be dominant since addition of the sterol results in an increase in P_t from 0.36 to 0.69 (the quadrupole splitting increases from 22.5 to 43.1 kHz). However, from the increase in P_t alone, we expect $\Delta T_1 > 1$, but we observe $\Delta T_1 = 0.51$. Thus, the increase in P_t is moderated by the second mechanism, since the long-axis diffusion rate becomes larger than the gauche–trans isomerization rate. Specifically, in going from 0 (Figure 2) to 40 mol % CHOL (Figure 3), k_{ax} increases by an order of magnitude to 2×10^{10} s^{-1}, and the gauche–trans isomerization rate decreases by an order of magnitude to 4×10^9 s^{-1}. A similar effect was noted by Siminovitch et al. (1988) in CHOL/DPPE bilayers. Thus, we see that addition of CHOL has a substantial ordering effect in that it increases the proportion of trans isomers in a chain. Concurrently, it slows the isomerization rate and greatly increases the axial diffusion rate. Together, these two effects lead to a change in ΔT_1 from −0.45 to 0.51.

The observation of orientation-dependent relaxation in the L_α phase of pure bilayers is somewhat of a surprise. In lecithin bilayers it was suggested that the T_1 anisotropy is obscured by fast lateral diffusion, which allows a lipid molecule to sample all orientations in a time comparable to T_1 (Brown & Davis, 1981), and it has been presumed that all pure lipid bilayers would show the same effects as pure lecithin. However, the recent report by Jarrell et al. (1988) that $\Delta T_1 = 0$ even in bilayers oriented on glass plates suggested that other mechanisms could be responsible for the vanishing T_1 anisotropy. Moreover, the data presented here, plus spectra of two other systems to be described elsewhere, suggest that anisotropic T_1's are probably a general feature of polymethylene chain motion in L_α-phase lipids. First, we have found a T_1 anisotropy in the L_α phase of NPSM where the upper parts of the chain show $\Delta T_1 > 0$. In contrast to NPGS, NPSM exhibits positive ΔT_1 down to at least the 7-position of the palmitoyl chain (J. B. Speyer, S. K. Das Gupta, P. K. Sripada, G. G. Shipley, and R. G. Griffin, unpublished results). Second, we have initiated studies on L_α-phase DPPC liposomes and noted a clear anisotropy with $\Delta T_1 > 0$ at the 3-position in the glycerol backbone and $\Delta T_1 < 0$ at the 12-position in the *sn*-2 acyl chain. This suggests that the reports by Brown and Davis (1981) and Jarrell et al. (1988) are probably special cases, such as we have observed in 4,4-d_2-NPGS, where $\Delta T_1 \simeq 0$, particularly since both of these employed lecithins labeled in the neighborhood of the 4-position. In light of our results on NPGS, NPSM, and glycerol- and chain-labeled DPPC and those of Jarrell et al. (1988), it appears that, while lateral diffusion may contribute to a vanishing T_1 anisotropy, it may not be the primary source of this effect. Clearly, it will be interesting to study partially relaxed spectra in a number of different lipid systems to characterize their dynamic behavior.

The physical origin of the sign change in ΔT_1 lies in the behavior of the spectral density functions J_1 and J_2, which, as shown in eq 3, determine T_1. For fast-limit axially symmetric line shapes, J_1 and J_2 contain terms proportional to $\cos^2\theta$ and $\cos^4\theta$ but are independent of ϕ (Torchia & Szabo, 1982), where θ and ϕ are the polar angles relating the symmetry axis to the magnetic field. For motional models involving jumps or diffusion about a symmetry axis, it has been shown (D. J. Siminovitch, private communication) that the J_1 and $4J_2$ terms containing $\cos^4\theta$ will always cancel. That $\Delta T_1 = 0$ in some cases such as at the 4-position of NPGS, or DMPC (Jarrell et al., 1988), and in the continuously diffusing methyl group (Torchia & Szabo, 1982) is due to the fortuitous cancellation of both the $\cos^2\theta$ and $\cos^4\theta$ terms. In the less extreme cases of the 3- and 12-positions of NPGS, the sign of the T_1 anisotropy is determined by the angular dependence of J_2, and the magnitude of the anisotropy is modulated by J_1.

Conclusions

We have shown that significant T_1 anisotropy exists in L_α-phase cerebroside and that the line shapes resulting from inversion recovery experiments are sensitive to motional rates and mechanisms. We have simulated the spectra in some detail using a simple model of discrete whole-molecule diffusion about the long axis coupled with gauche–trans isomerization. By measuring the T_1 anisotropy at several sites, constraints are imposed on the rates of axial diffusion, thus providing a means to determine k_{gt} and P_t of each position. Addition of cholesterol has the effect of increasing the probablity of trans conformers and slowing the rate of gauche–trans isomerization, while increasing the rate of molecular reorientation about the lipid long axis. The rates obtained from the simulations are in general agreement with rates in other lipid systems obtained with other techniques and models. Preliminary studies of other L_α-phase lipids (NPSM and DPPC) indicate our approach is probably widely applicable, and it greatly extends the range of motions that are open to analysis through NMR.

Acknowledgments

We thank D. J. Siminovitch, H. C. Jarrell, D. A. Torchia, and J. H. Davis for several stimulating conversations. We also thank J. Seelig for providing the glycerol-labeled DPPC.

References

Auger, M., Carrier, D., Smith, I. C. P., & Jarrell, H. C. (1989) *J. Am. Chem. Soc.* (submitted for publication).
Batchelder, L. S., Niu, C. H., & Torchia, D. A. (1983) *J. Am. Chem. Soc. 105*, 2228.
Beshah, K., & Griffin, R. G. (1989) *J. Magn. Reson. 84*, 268.
Beshah, K., Olejniczak, E. T., & Griffin, R. G. (1987) *J. Chem. Phys. 86*, 4730.
Bloom, M., Davis, J. H., & Valic, M. I. (1980) *Can. J. Phys. 58*, 1510.
Blume, A., & Griffin, R. G. (1982) *Biochemistry 21*, 6230.
Blume, A., Rice, D. M., Wittebort, R. J., & Griffin, R. G. (1982) *Biochemistry 21*, 6220.
Bonmatin, J.-M., Smith, I. C. P., Jarrell, H. C., & Siminovitch, D. J. (1988) *J. Am. Chem. Soc. 110*, 8693.
Bonmatin, J.-M., Smith, I. C. P., Jarrell, H. C., & Siminovitch, D. J. (1989) *J. Am. Chem. Soc.* (submitted for publication).
Brown, M. F. (1982) *J. Chem. Phys. 77*, 1576.
Brown, M. F., & Davis, J. H. (1981) *Chem. Phys. Lett. 79*, 431.
Brown, M. F., Ribeiro, A. A., & Williams, G. D. (1983) *Proc. Natl. Acad. Sci. U.S.A. 80*, 4325.
Charvolin, J., Manneville, P., & Deloche, B. (1973) *Chem. Phys. Lett. 23*, 345.
Das Gupta, S. K., Rice, D. M., & Griffin, R. G. (1982) *J. Lipid Res. 23*, 197.
Davis, J. H. (1983) *Biochim. Biophys. Acta 73*, 117.
Doane, J. W., Tarr, C. E., & Nickerson, M. A. (1974) *Phys. Rev. Lett. 33*, 620.

Fuson, M. M., & Prestegard, J. H. (1983) *Biochemistry 22*, 1311.
Gally, H. U., Pluschke, G., Overath, P., & Seelig, J. (1981) *Biochemistry 20*, 1826.
Griffin, R. G., Beshah, K., Ebelhäuser, R., Huang, T. H., Olejniczak, E. T., Rice, D. M., Siminovitch, D. J., & Wittebort, R. J. (1988) *The Time Domain in Surface and Structural Dynamics* (Long, G. J., & Grandjean, F., Eds.) pp 81-105, Kluwer Academic Publishers, Dordrecht, The Netherlands.
Hiyama, Y., Silverton, J. V., Torchia, D. A., Grieg, J. T., & Hammond, S. J. (1986) *J. Am. Chem. Soc. 108*, 2715.
Huang, T. H., Skarjune, R. P., Wittebort, R. J., Griffin, R. G., & Oldfield, E. (1980) *J. Am. Chem. Soc. 102*, 7377.
Jarrell, H. C., Smith, I. C. P., Jovall, P. A., Mantsch, H. H., & Siminovitch, D. J. (1988) *J. Chem. Phys. 88*, 1260.
Lange, A., Marsh, D., Wassmer, K.-H., Meier, P., & Kothe, G. (1985) *Biochemistry 24*, 4384.
Mayer, C., Müller, K., Weisz, K., & Kothe, G. (1988) *Liq. Cryst. 3*, 797.
Meier, P., Ohmes, E., Kothe, G., Blume, A., Weidner, J., & Eibl, H. J. (1983) *J. Phys. Chem. 87*, 4904.
Meier, P., Ohmes, E., & Kothe, G. (1986) *J. Chem. Phys. 85*, 3598.
Petersen, N. O., & Chan, S. I. (1977) *Biochemistry 16*, 2657.
Radin, N. S. (1972) *Methods Enzymol. 28*, 300.
Rice, D. M., Meinwald, V. C., Scheraga, H. A., & Griffin, R. G. (1987) *J. Am. Chem. Soc. 109*, 1636.
Rommel, E., Noack, F., Meier, P., & Kothe, G. (1988) *J. Phys. Chem. 92*, 2981.
Ruocco, M. J., & Shipley, G. G. (1984) *Biophys. J. 46*, 695.
Seelig, J. (1977) *Q. Rev. Biophys. 10*, 353.
Seelig, A., & Seelig, J. (1974) *Biochemistry 13*, 4839.
Siminovitch, D. J., Olejniczak, E. T., Ruocco, M. J., Das Gupta, S. K., & Griffin, R. G. (1985) *Chem. Phys. Lett. 119*, 251.
Siminovitch, D. J., Ruocco, M. J., Olejniczak, E. T., Das Gupta, S. K., & Griffin, R. G. (1988) *Biophys. J. 54*, 373.
Spiess, H. W., & Sillescu, H. (1981) *J. Magn. Reson. 42*, 381.
Torchia, D. A., & Szabo, A. (1982) *J. Magn. Reson. 49*, 107.
Williams, G. D., Beach, J. M., Dodd, S. W., & Brown, M. F. (1985) *J. Am. Chem. Soc. 107*, 6868.
Wittebort, R. J., Olejniczak, E. T., & Griffin, R. G. (1987) *J. Chem. Phys. 86*, 5411.

Articles

Thermostability of Cytochrome *c*-552 from the Thermophilic Hydrogen-Oxidizing Bacterium *Hydrogenobacter thermophilus*†

Yoshihiro Sanbongi, Yasuo Igarashi, and Tohru Kodama*

Department of Agricultural Chemistry, University of Tokyo, Bunkyo-ku, Tokyo 113, Japan

Received May 1, 1989; Revised Manuscript Received August 9, 1989

ABSTRACT: The denaturation of the *c*-type cytochrome of the thermophilic bacterium *Hydrogenobacter thermophilus* cytochrome *c*-552 by heat and guanidine hydrochloride was studied by measuring the change in circular dichroic spectra. The melting temperature ($T_{1/2}$) of cytochrome *c*-552 in the presence of 1.5 M guanidine hydrochloride was 34 °C higher than that of the *c*-type cytochrome of *Pseudomonas aeruginosa* cytochrome *c*-551. *Hydrogenobacter* cytochrome *c*-552 is a much more stable protein than cytochrome *c*-551 of the mesophilic bacterium *P. aeruginosa*, even though their amino acid sequences are 56% identical and they have numerous other similarities. However, notwithstanding these similarities between the sequences of the cytochromes *c*-552 and *c*-551 that were compared, it is very likely that these differences in stability could be due to some heretofore undefined differences in their spatial structures. It has been suggested that α-helix structure and electrostatic interaction could be the source of the stable spatial structure of cytochrome *c*-552.

Hydrogenobacter thermophilus TK-6 (IAM 12695) produces a large amount of cytochrome *c*-552 within its cell structure and also in a culture broth (Ishii et al., 1987a). Cytochrome *c*-552 reacts with hydrogenase isolated from *H. thermophilus* TK-6, which is considered to be the first reaction in the electron flow in this hydrogen-oxidizing microorganism (Ishii et al., 1987b). Also, cytochrome *c*-552 has a molecular weight of 7600, which is believed to be the lowest molecular weight among bacterial cytochromes *c* ever reported (Ishii et al., 1987a).

We determined the whole amino acid sequence of cytochrome *c*-552 derived from *H. thermophilus* in a previous paper (Sanbongi et al., 1989). *Hydrogenobacter* cytochrome *c*-552 consists of 80 amino acid residues, and its amino acid sequence closely resembles that of cytochrome *c*-551 from *Pseudomonas aeruginosa*, which consists of 82 amino acid residues. However, cytochrome *c*-552 from an extreme thermophilic *H. thermophilus* is believed to be more stable in heat than cytochrome *c*-551 from a mesophilic bacterium, *P. aeruginosa*. Perutz and Raidt (1975) attempted to specify the amino acid residues contributing to thermostability. They

† This work was supported in part by Grant-in Aid for Scientific Research 62470122 from the Ministry of Education, Science and Culture of Japan.

* Correspondence should be addressed to this author.

0006-2960/89/0428-9574$01.50/0